Computational integral imaging reconstruction by use of scale-variant magnification technique

Dong-Hak Shin and Hoon Yoo
Dept. of Visual Contents, Dongseo University, Pusan, 617-716, Korea
TEL:82-51-320-1734, e-mail: hunie@dongseo.ac.kr.

Keywords : 3D display, integral imaging, image reconstruction, lenslet array

Abstract

In this paper, we present an interference problem among elemental images in computational integral imaging reconstruction. To overcome the interference problem, we propose a method to calculate a minimum magnification factor and the preliminary experiments are performed.

1. Introduction

Integral imaging has been attractive techniques [1-6] for autostereoscopic three-dimensional (3D) display due to the merits such as full parallax, continuous viewing angle and full color display. In general, an integral imaging system consists of two parts; pickup and reconstruction. In the pickup part, rays emanating from a 3D object passing through a lenslet array are recorded as elemental images that represent different perspectives of a 3D object.

On the other hand, two kinds of reconstruction methods have been studied for volumetric 3D image display in the reconstruction part. One is an optical reconstruction (OR) method [2-6] and the other is a computational integral imaging reconstruction (CIIR) method [7-12]. Among them, in 2004, a CIIR method based on a pinhole array model has been introduced [7]. The principle of the conventional CIIR method is shown in Fig. 1(a). First, an elemental image is projected inversely through the corresponding pinhole. When an image is produced on a reconstructed output plane (ROP), the inversely projected elemental image is digitally magnified by a magnification factor $M=z/g$, where z is the distance between the virtual pinhole array and the ROP and g is the distance between the pinhole array and the elemental image plane, respectively. Second, the magnified elemental images are overlapped on the ROP. Next the normalization process is required to reduce an artifact [9]. To completely reconstruct a reconstructed plane image (RPI) of a 3D object at the distance of z, these three processes must be repeatedly performed with respect to the entire elemental images. The iterative computation of the above three processes provides a series of z-dependent RPIs. Recently, CIIR-based computational integral imaging has been applied to useful applications such as object recognition and a 3D correlator [10-11].

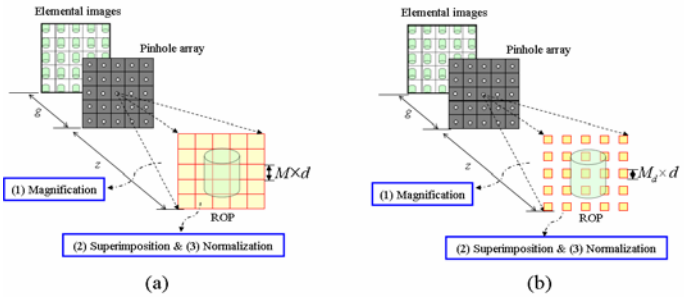

Fig. 1. Principle of the CIIR (a) Conventional method (b) Proposed method.

In the conventional CIIR method, there are some serious problems to be solved. For example, there are artifacts that reconstructed images have and the high computational load that is due to a large magnification factor at far distance. In addition, images that reconstructed by the CIIR method suffer from blurring although it is reconstructed at the right position where a 3D object is located. This is because the overlapping process of the conventional CIIR method incurs interference among adjacent pixels when magnified elemental images are superimposed on each other. Actually, the interference prevents CIIR from reconstructing high resolution images for 3D objects.

In this paper, to overcome the interpixel interference problem, we propose scale-variant magnification (SVM) for CIIR. We first explain the

interpixel interference problem in CIIR. Minimizing the interpixel interference enables CIIR to provide resolution-enhanced plane images.

2. Proposed CIIR method using SMT

Figure 1(b) illustrates the principle of the proposed CIIR method using SVM. CIIR consists of three processes: magnification, superposition, and normalization. The main difference between the conventional CIIR method and our method is that our method uses a new magnification factor $M_d(z)$ to reduce interference between adjacent pixels in the superposition process.

To understand the interference problem in the conventional CIIR method, we consider a computational integral imaging system for a point object as shown in Fig. 2. Figure 2(a) shows that a point object is recorded with a lenslet array to be elemental images. Now, consider a pixel-to-pixel mapping between pixels of elemental images and pixels in ROP without magnification as shown in Fig. 2(b). Here, we call the mapped pixels in ROP as effective pixels. The number of effective pixels is the same to that of elemental images. However, the size of domain of ROP increases as the distance z increases. Thus, there may be empty area in ROP. In the conventional CIIR method, effective pixels are magnified by a magnification factor $M=z/g$ and then the magnified pixels are superimposed on ROP, as shown in Fig. 2(c). In this case, the reconstructed image of the point object can be obtained on the ROP at the position where the point object is placed. The superposition of the magnified pixels fills the empty space smoothly. However, effective pixels are interfered with each other due to the large magnification. Note that effective pixels represent the component pixels of 3D objects and have the exact intensity value of 3D objects. Thus, they should not be overlapped to obtain a high resolution image.

To avoid this interference problem, we propose a SVM technique in CIIR. We design a new magnification factor $M_d(z)$ with respect to the distance z in order that magnified pixels are unable to interfere their adjacent effective pixels. Figure 2(d) shows each pixel of elemental images is magnified by a factor of $M_d(z)$ in the magnification process. The factor $M_d(z)$ can be determined to be the distance between the two nearest effective pixels.

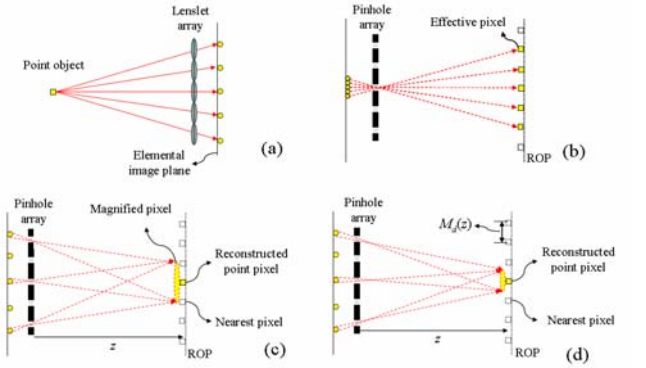

Fig. 2. (a) Pickup (b) Pixel-to-pixel mapping (c) Conventional CIIR method (d) Proposed CIIR method.

To calculate a factor $M_d(z)$ with respect to z, we consider a ray diagram that shows rays emanating from the elemental images and passing through the pinholes as shown in Fig. 3(a). In order to formulate the relation between elemental images and a RPI, we use the ray analysis using the ABCD matrix [6]. In Fig 3(a), we assume the use of a pinhole array with K pinholes and consider only the rays starting from pixels of the elemental images and passing through each pinhole. Each elemental image region corresponding to each pinhole has N pixels. If n-th ray passing through the k-th pinhole reaches the ROP at z, it is represented by

$$H_n^k(z) = kp - \frac{z}{g}nd \tag{1}$$

Now, to calculate the distance between the two effective pixels in ROP, we consider two rays in ROP as shown in Fig. 3(a). The first ray comes from the n_1-th pixel of the k_1-th elemental image and the second ray comes from the n_2-th pixel of the k_2-th elemental image. Then the distance between two rays in ROP is given by

$$\Delta H = H_{n_2}^{k_2}(z) - H_{n_1}^{k_1}(z) = p(k_2 - k_1) - \frac{z}{g}(n_2 - n_1)d \tag{2}$$

Note that $\Delta H=0$ means the two rays are overlapped at the same point. If $\Delta H\neq 0$, there is an empty area that should be filled with pixels. The number of pixels to be inserted between the two rays is obtained by

$$\alpha = \frac{\Delta H}{d} = N(k_2 - k_1) - M(n_2 - n_1) \tag{3}$$

Here, $0 < |k_2-k_1| < K$ and $0 < |n_2-n_1| < N$. Using Eq. (3),

we can select the minimum integer value of α by calculating (k_2-k_1) and (n_2-n_1) values for entire elemental images. The minimum value α means the minimum number of pixels to be inserted between the two adjacent effective pixels in ROP. We use this minimum value α as a new magnification factor M_d in the proposed method.

Candidates for the new magnification factor are calculated by using Eq. (3) with respect to z and then minimum value among the candidates is selected as a factor M_d with respect to z. An example for the factor M_d is shown in Fig. 3(b), where N=34 and K=30. This result indicates that M_d is variant with respect to z. It is much smaller than conventional magnification factor M except for z=51 mm. The exceptional case is where many rays are overlapped at the same point. In fact, the magnification factor used in CIIR is linearly proportional to computational costs. The larger magnification factor spends more memories and computation time. Thus, the proposed method is considered to be (M/M_d) times faster than the previous method. For example of Fig. 3(b), we can obtain improvement of 49 times when z=21 mm.

In the superposition process, the elemental images magnified by a new factor of M_d are superimposed on ROP to generate a RPI. Here the proposed method eliminates the interference problem between adjacent effective pixels as explained in Fig. 2. In fact, the interference between adjacent pixels produces a blurred RPI. Thus the proposed method provides accurate reconstruction of 3D objects because the blurring is reduced. Finally, the RPI is normalized by the number of signals overlapped.

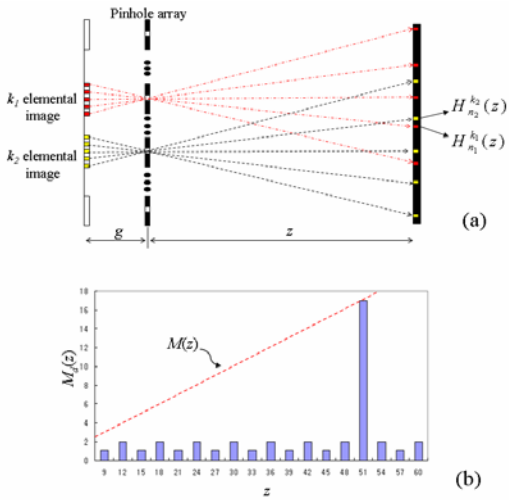

Fig. 3. (a) Ray formation of proposed CIIR method. (b) Comparison of $M(z)$ and $M_d(z)$.

3. Experimental results

To show the effectiveness of our proposed CIIR method, computational experiments on the reconstruction of three test images were performed. The experimental structure is shown in Fig. 4(a). The pinhole array in the experimental setup is composed of 30×30 pinholes and it is located at z=0 mm. The interval between pinholes is 1.08 mm and the gap g between the elemental images and the pinhole array is 3 mm. Three images named Lena, Car, and Cow are used as test images, as shown in Fig. 4(b). The size of each image is 1020×1020 pixels. After a test image is located at distance z, its elemental images are synthesized by computational pickup based on the simple ray geometric analysis [6]. The number of each elemental image that has 34×34 pixels is 30×30. And then the synthesized elemental images are used in the CIIR methods. In our CIIR method (where N =34 and K =30), elemental images are magnified by a factor of M_d(z), as shown in Fig. 3(b), and are summated on the ROP at z to reconstruct a RPI. Finally, the RPI is normalized by the number of elemental images overlapped. Therefore the final RPI at z was obtained.

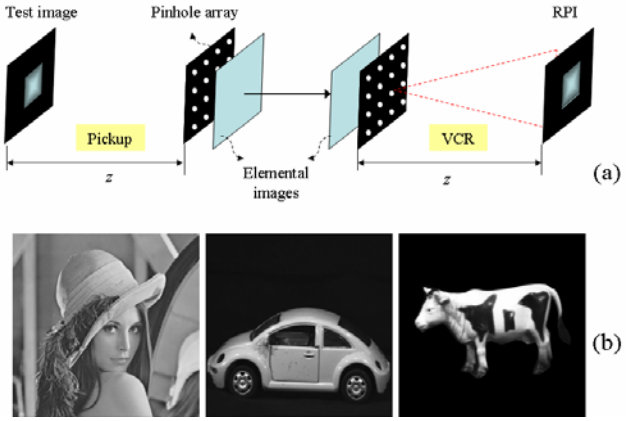

Fig. 4. (a) Experimental structure. (b) Three test images.

To quantitatively evaluate our resolution-enhanced CIIR method, the peak signal-to-noise ratio (PSNR) is employed as an image quality measure [12]. For the three test images, the average PSNR is calculated according to the distance z. The PSNR results are presented in Fig. 5. As z increases, the PSNR of the conventional method decreases due to the increasing interference for a large value M. However, our method depends on not M but M_d(z). These PSNR results indicate that the proposed method improves image

quality on the average 7.01dB when it is compared with the conventional method. Figure 6(a) and 6(b) show the examples of the RPIs in the best case z=21 mm and the worst case z=51 mm for both the conventional method and the proposed method, respectively. It is seen that a perfect reconstruction of the original test image, as shown in Fig. 6, can be obtained in the best case z=21 mm (M_d =1). However the worst case shows the same visual quality of the image reconstructed from the conventional method because the magnification factor is the same (M= M_d =17).

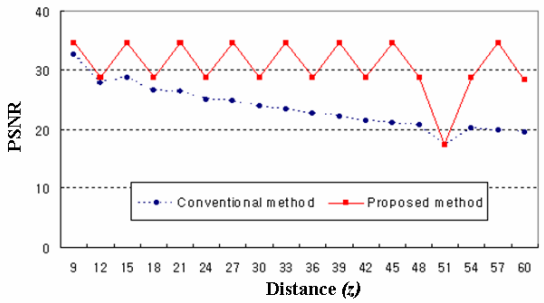

Fig. 5. Average PSNR results for three test images.

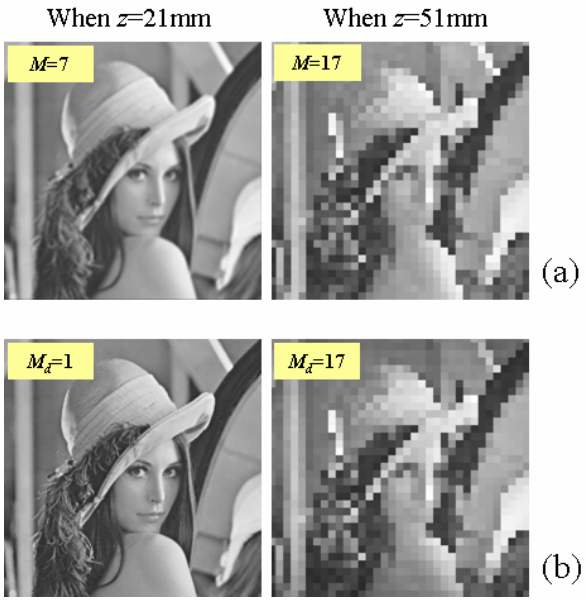

Fig. 6. Comparison of reconstructed images (a) Conventional method (b) Proposed method.

4. Conclusions

We have proposed a resolution-enhanced CIIR method using SVM. In this paper we introduced the interference problem that the magnification by a large factor causes in the superposition process of CIIR. To overcome the interference problem, the magnification factor is required to be minimized. Based on this, we proposed a method to calculate the minimum magnification factor. Computational experiments indicate that new magnification factor enables the proposed method to reconstruct resolution-enhanced images. In addition, it provides us a fast calculation of CIIR compared with the conventional method. Therefore, we expect that the proposed CIIR method may be usefully applied to 3D pattern recognition.

5. References

1. G. Lippmann, *C.R. Acad. Sci.*, **146**, 446 (1908).
2. F. Okano, H. Hoshino, J. Arai, and I. Yuyama, *Opt. Eng.*, **38**, 1072 (1999).
3. J.-S. Jang and B. Javidi, *Opt. Lett.*, **27**, 324 (2002).
4. B. Lee, S. Y. Jung, S.-W. Min, and J.-H. Park, *Opt. Lett.*, **26**, 1481 (2001).
5. M. Martínez-Corral, B. Javidi, R. Martínez-Cuenca, and G. Saavedra, *J. Opt. Soc. Am. A*, **22**, 597 (2005).
6. D.-H. Shin, B. Lee, and E.-S. Kim, *Appl. Opt.*, **45**, 7375 (2006).
7. S.-H. Hong, J.-S. Jang, and B. Javidi, *Opt. Express*, **12**, 483 (2004).
8. D.-H. Shin, E.-S. Kim and B. Lee, *Jpn. J. Appl. Phys.*, **44**, 8016-8018 (2005).
9. S.-H. Hong and B. Javidi, *Opt. Express*, **12**, 4579 (2004).
10. B. Javidi, R. Ponce-Díaz, and S. -H. Hong, *Opt. Lett.*, **31**, 1106 (2006)
11. J.-S. Park, D.-C. Hwang, D.-H. Shin and E.-S. Kim, *Opt. Commun.*, **276**, 72 (2007).
12. D.-H. Shin and H. Yoo, *Opt. Express*, **16**, 8855 (2008).